Supporting Information

Dynamics and Location of the Allosteric Midazolam Site in Cytochrome P4503A4 in Lipid Nanodiscs

Michelle Redhair[1], John C Hackett*[,2], Robert D. Pelletier[1], William M. Atkins*[,1]

[1]Department of Medicinal Chemistry, University of Washington, Seattle, Washington 98195-7610
[2]Department of Physiology and Biophysics and the Massey Cancer Center, School of Medicine, Virginia Commonwealth University, Richmond, Virginia 23298-0035
*corresponding author: winky@uw.edu; john.hackett@vcuhealth.org

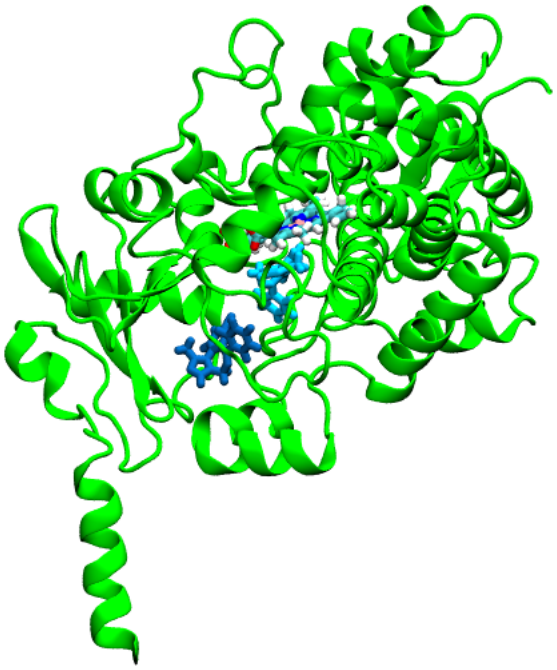

Figure S1. Initial position of the second MDZ (dark blue) for two-MDZ simulations.

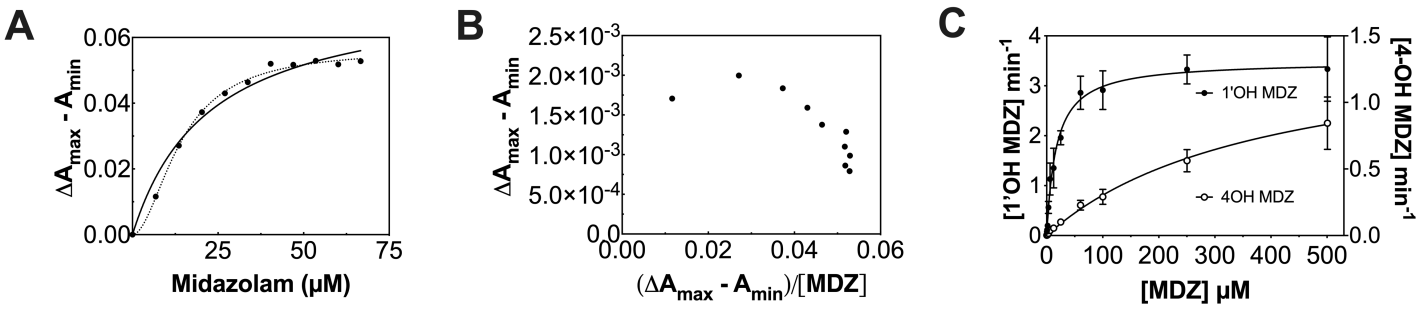

Figure S2. Equilibrium binding data. A) The dashed line shows the fit of the binding data to the hill equation. The black line shows the fit to the Michaelis-Menten equation. B) Eadie-Hofstee plot for MDZ binding to CYP3A4 ND. C) Midazolam hydroxylation kinetics. Product formation (nmole product / nmole CYP3A4 / min, or min^{-1}) are plotted vs MDZ concentration (μM). The closed and open circles represent 1'OH MDZ and 4OH-MDZ product formation, respectively.

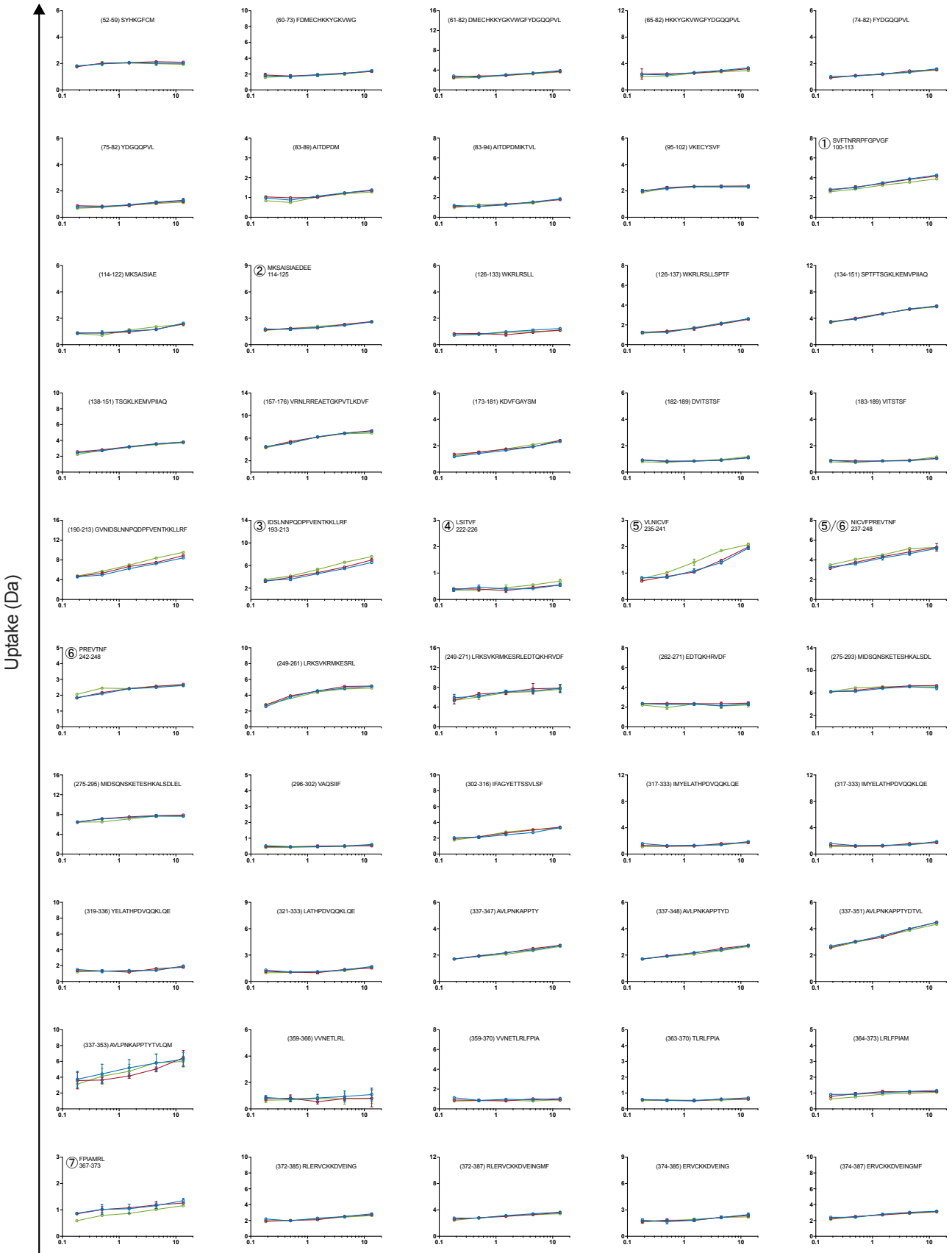
(52-59) SYHKGFCM
(60-73) FDMECHKKYGKVWG
(61-82) DMECHKKYGKVWGFYDGQQPVL
(65-82) HKKYGKVWGFYDGQQPVL
(74-82) FYDGQQPVL
(75-82) YDGQQPVL
(83-89) AITDPDM
(83-94) AITDPDMIKTVL
(95-102) VKECYSVF
① SVFTNRRPFGPVGF 100-113
(114-122) MKSAISIAE
② MKSAISIAEDEE 114-125
(126-133) WKRLRSLL
(126-137) WKRLRSLLSPTF
(134-151) SPTFTSGKLKEMVPIIAQ
(138-151) TSGKLKEMVPIIAQ
(157-176) VRNLRREAETGKPVTLKDVF
(173-181) KDVFGAYSM
(182-189) DVITSTSF
(183-189) VITSTSF
(190-213) GVNIDSLNNPQDPFVENTKKLLRF
③ IDSLNNPQDPFVENTKKLLRF 193-213
④ LSITVF 222-226
⑤ VLNICVF 235-241
⑤/⑥ NICVFPREVTNF 237-248
⑥ PREVTNF 242-248
(249-261) LRKSVKRMKESRL
(249-271) LRKSVKRMKESRLEDTQKHRVDF
(262-271) EDTQKHRVDF
(275-293) MIDSQNSKETESHKALSDL
(275-295) MIDSQNSKETESHKALSDLEL
(296-302) VAQSIIF
(302-316) IFAGYETTSSVLSF
(317-333) IMYELATHPDVQQKLQE
(317-333) IMYELATHPDVQQKLQE
(319-336) YELATHPDVQQKLQE
(321-333) LATHPDVQQKLQE
(337-347) AVLPNKAPPTY
(337-348) AVLPNKAPPTYD
(337-351) AVLPNKAPPTYDTVL
(337-353) AVLPNKAPPTYTVLQM
(359-366) VVNETLRL
(359-370) VVNETLRLFPIA
(363-370) TLRLFPIA
(364-373) LRLFPIAM
⑦ FPIAMRL 367-373
(372-385) RLERVCKKDVEING
(372-387) RLERVCKKDVEINGMF
(374-385) ERVCKKDVEING
(374-387) ERVCKKDVEINGMF
Uptake (Da)
Time (min)

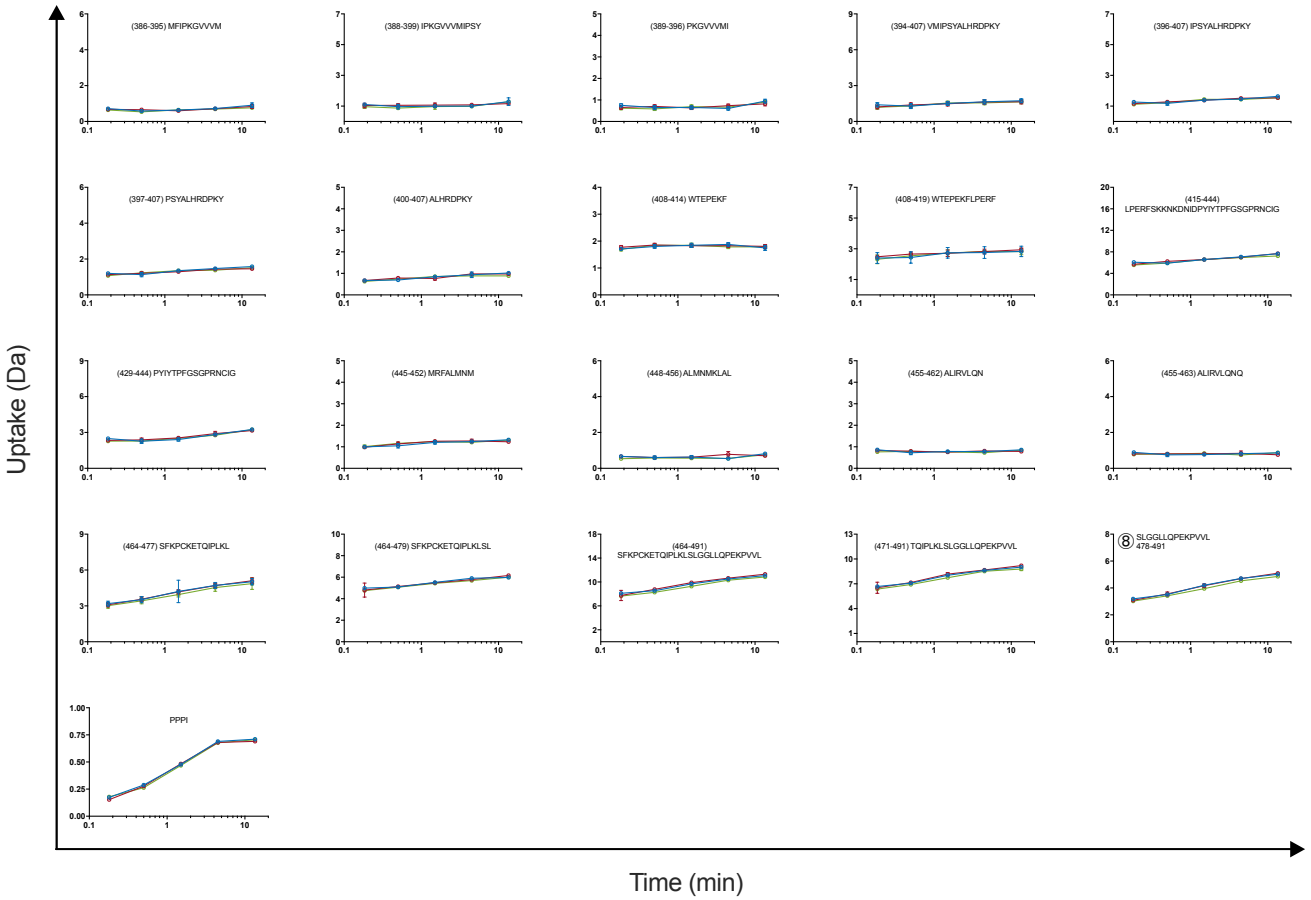

Figure S3. Deuterium uptake (Da) vs Time (min) plots for each peptide. Exchange for the 0 μM, 6 μM and 60 μM MDZ samples is shown in blue, red, and green open circles, respectively. The error bars represent the standard deviation from duplicate experiments.

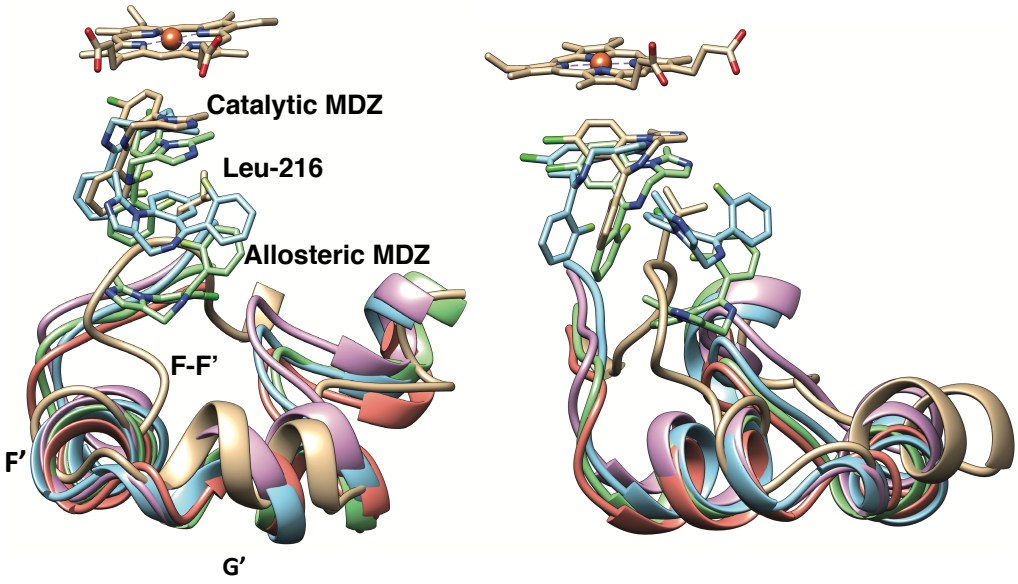

Figure S4: Two views depicting comparisons of the F-G regions in the 5TE8 structure (tan) with the endpoints of the four GaMD simulations (blue, green, pink and orange) with two MDZ molecules bound. Representative MDZ positions from two of the four GaMD snapshots are depicted for clarity. The F-F' loop of the 5TE8 structure, specifically in the vicinity of Leu-216, occupies the same space as the predicted MDZ allosteric site. Binding of the allosteric MDZ is prohibited in the 5TE8 structure due to steric clash with the F-F' loop, but allowed upon addition of two MDZ's to the ligand free structure.

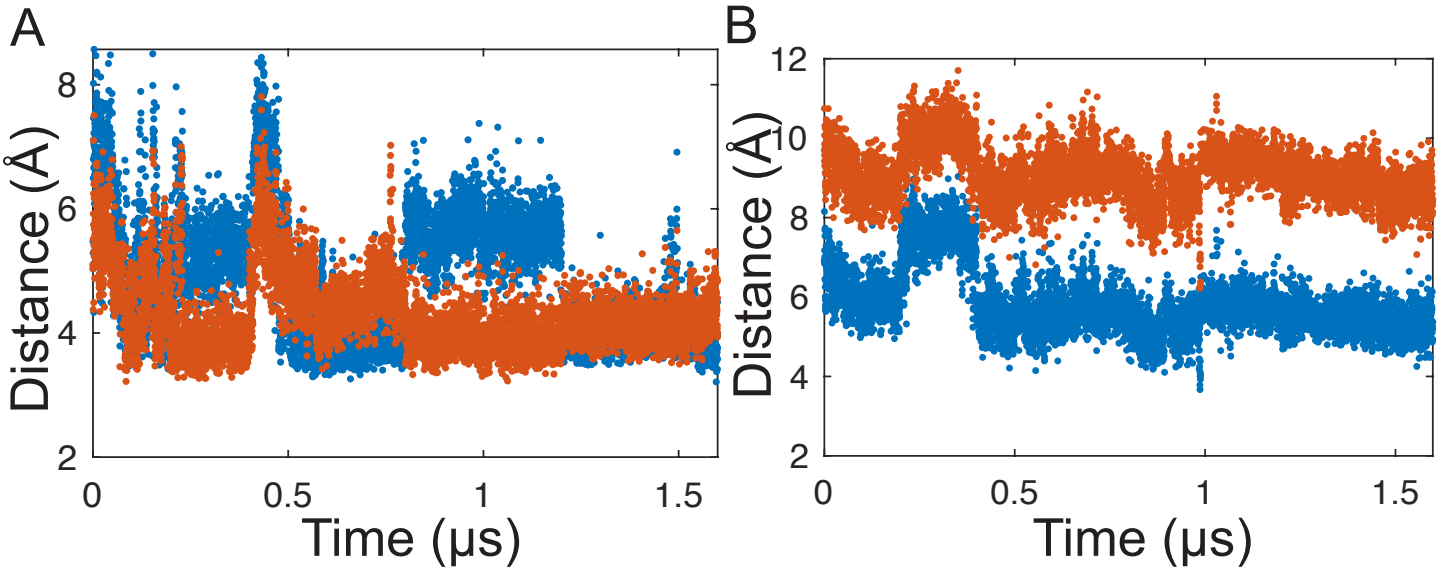

Figure S5. Distances between the Arg-105 Cζ and the MDZ1 N5 (blue) and center of the MDZ1 fluorophenyl ring (orange) when one (A) and two (B) MDZ molecules are present in the CYP3A4 active site.